Molecular characterization and functional properties of cardiomyocytes derived from human inducible pluripotent stem cells

Igal Germanguz [a, b, #], Oshra Sedan [a, b, c, #], Naama Zeevi-Levin [a, b, #], Ronit Shtrichman [a, b, #], Efrat Barak [a, b, #], Anna Ziskind [a, b], Sivan Eliyahu [a, b, c], Gideon Meiry [a, b, c], Michal Amit [a, b], Joseph Itskovitz-Eldor [a, b, d], Ofer Binah[a, b, c, *]

[a] The Sohnis Family Stem Cells Center, Technion – Israel Institute of Technology, Haifa, Israel
[b] Ruth & Bruce Rappaport Faculty of Medicine, Technion – Israel Institute of Technology, Haifa, Israel
[c] The Rappaport Family Institute for Research in the Medical Sciences, Technion – Israel Institute of Technology, Haifa, Israel
[d] Rambam Medical Center, Haifa, Israel

Received: June 19, 2009; Accepted: December 3, 2009

Abstract

In view of the therapeutic potential of cardiomyocytes derived from induced pluripotent stem (iPS) cells (iPS-derived cardiomyocytes), in the present study we investigated in iPS-derived cardiomyocytes, the functional properties related to $[Ca^{2+}]_i$ handling and contraction, the contribution of the sarcoplasmic reticulum (SR) Ca^{2+} release to contraction and the β-adrenergic inotropic responsiveness. The two iPS clones investigated here were generated through infection of human foreskin fibroblasts (HFF) with retroviruses containing the four human genes: OCT4, Sox2, Klf4 and C-Myc. Our major findings showed that iPS-derived cardiomyocytes: (*i*) express cardiac specific RNA and proteins; (*ii*) exhibit negative force–frequency relations and mild (compared to adult) post-rest potentiation; (*iii*) respond to ryanodine and caffeine, albeit less than adult cardiomyocytes, and express the SR-Ca^{2+} handling proteins ryanodine receptor and calsequestrin. Hence, this study demonstrates that in our cardiomyocytes clones differentiated from HFF-derived iPS, the functional properties related to excitation–contraction coupling, resemble in part those of adult cardiomyocytes.

Keywords: induced pluripotent stem cells • cardiomyocytes • calcium transients • contractions • Beta adrenergic responsiveness • sarcoplasmic reticulum

Introduction

Cardiovascular diseases including myocardial infarction and heart failure are the most frequent causes of death in the industrialized world. While the current pharmacotherapy for congestive heart failure (which includes angiotensin converting enzyme inhibitors and β-blockers) improves clinical outcome, these treatment modalities as well as various interventional and surgical therapeutic methods have limited efficacy because of their inability to repair or replace damaged myocardium. Given the high morbidity and mortality rates associated with these major diseases, shortage of donor hearts for transplantation, complications resulting from immunosuppression and long-term failure of transplanted organs [1, 2], novel therapeutic means for improving cardiac function and preventing heart failure are in critical demand. Regeneration or repair of the damaged myocardium can be accomplished by the use of cell therapy, which is the transplantation of healthy, functional and propagating cells to restore the viability or function of deficient tissues [3–5]. In this regard, many studies have shown that improvement of myocardial function can be achieved in experimental animal models of heart failure and infarction, by transplanting embryonic stem cells-derived cardiomyocytes into the compromised myocardium [6–8].

A novel potential source for cardiac cell regeneration is cardiomyocytes derived from human inducible pluripotent stem (iPS) cells generated from skin fibroblasts. Hence, thanks to the

[#]These authors contributed equally to the manuscript.
*Correspondence to: Ofer BINAH, Department of Physiology, Ruth & Bruce Rappaport Faculty of Medicine, 1 Efron Street, Bat-Galim, P.O.Box 9649, Haifa 31096, Israel.
Tel.: +972-4-8295262
Fax: +972-4-8513919
E-mail: binah@tx.technion.ac.il

doi:10.1111/j.1582-4934.2009.00996.x

© 2011 The Author
Journal of Cellular and Molecular Medicine © 2011 Foundation for Cellular and Molecular Medicine/Blackwell Publishing Ltd

breakthrough inventions of Yamanaka and coworkers [9, 10] 'producing' human cardiomyocytes from different sources has now become an attractive viable option. In principle, this group generated iPS cells from mouse and human somatic cells, by introducing these cells with four factors: Oct3/4, Sox2, Klf4 and c-Myc, thus reprogramming somatic cells to pluripotent stem cells. Briefly, the resulting iPS cells were found to be similar to human embryonic stem cells (hESC) in morphology, proliferation, surface antigens, gene expression, epigenetic status and telomerase activity. Furthermore, these cells can differentiate *in vitro* into cell types of the three germ layers, and generate teratomas. Importantly, these studies have opened an avenue to generate cardiomyocytes from healthy human beings as well as from individuals with congenital heart diseases (*e.g.* familial hypertrophy), which will be very useful for understanding disease mechanisms, drug screening and toxicology studies [10].

In order to improve the prospects of cardiac cell transplantation, it is widely realized that the functional properties as well as the hormonal and pharmacological responsiveness of iPS-derived cardiomyocytes (iPS-CM) should be thoroughly investigated. Since it is preferred that the transplanted cells fully integrate within the malfunctioning myocardium, contribute to its contractile performance and respond appropriately to various stimuli (*e.g.* β-adrenergic stimulation), it is important to decipher their compatibility with the host myocardium. Since thus far, only the basic electrophysiological properties (at the action potential level) of iPS-CM were studied [11, 12], the aim of this study was to investigate in this unique preparation the functional properties related to intracellular Ca^{2+} handling, the role of the SR in the contraction process as well as β-adrenergic responsiveness. Our novel findings show that the clones of iPS-CM investigated in the present study, exhibit at least a partially functional SR (resembling in some aspects the adult myocardium), as well as positive inotropic responsiveness to β-adrenergic stimulation. In view of the therapeutic promise of iPS-CM, these cells should be further investigated as a potential source for cardiac cell therapy.

Methods

Establishing the reprogramming system

Generation of inducible pluripotent stem cells

iPS cells were generated from human foreskin fibroblasts (HFF) as previously described [9, 10]. HFF cells derived from a healthy male foreskin were purchased from ATCC (http://www.atcc.org). HFF cells were grown in fibroblasts medium containing Dulbecco's modified Eagle's medium (DMEM) supplemented with 10% foetal bovine serum (FBS, Hyclone, Logan, UT, USA) and 1 mM L-glutamine (Biological Industries, Beit Haemek, Israel). Four reprogramming constructs were obtained from AddGene (http://www.addgene.org), and include pMXs – Oct4 (17217, Shinya Yamanaka), pMXs-Sox2 (17218, Shinya Yamanaka), pMXs-Klf4 (17219, Shinya Yamanaka), pMXs- c-Myc (17220, Shinya Yamanaka). One hundred thousand HFF cells were infected with a supernatant mix of the four reprogramming retroviruses in two consecutive rounds [9]. Three days following infection the HFF cells were transferred onto fibronectin-coated dishes in mouse embryonic fibroblast (MEF) conditioned medium [13]. Two weeks later, the medium was changed to hESC-supporting medium containing 80% DMEM/F12 (Biological Industries) 20% knockout serum replacement, 8 ng/ml basic fibroblast growth factor, 1 mmol/l L-glutamine, 0.1 mmol/l β-mercaptoethanol and 1% non-essential amino acid stock (all from Gibco-BRL, Gaithersburg, MD, USA). Twenty-four days after infection, the few emerging morphologically embryonic stem cells (ESC)-like colonies were mechanically isolated. Each clone was grown separately on inactivated MEF-covered plates and was expanded as described for hESC [14].

Differentiating iPS colonies to cardiomyocytes

The iPS cells were cultured and differentiated using the same protocol used for the culture and differentiation of hESC [15]. Briefly, iPS cells from clones 1 and 2 were grown on inactivated MEF feeders in the same medium detailed in previous section. To induce embryoid bodies (EBs) formation, iPS cells were detached using 0.2% type IV collagenase (Worthington Biochemical, Lakewood, NJ, USA) and suspended in Petri dishes to allow their aggregation. Resultant EBs were grown in 80% DMEM (Gibco-BRL), 20% FBS (Hyclone), 1 mmol/l L-glutamine and 1% non-essential amino acid stock (both from Gibco-BRL). The EBs were then cultured in suspension for 7 days and subsequently plated on 0.1% gelatine-coated (Sigma-Aldrich, Rehorot, Israel) 6-well plates, during which spontaneously contracting EBs were observed.

Dissociation of contracting EBs

To increase the accessibility of cardiomyocytes to ryanodine and caffeine, spontaneously contracting EBs were micro-sectioned, dissociated and adhered onto 30-mm-diameter fibronectin-coated glass slides (Biological Industries). For the dissociation, the EBs were washed once with phosphate buffered saline (PBS) lacking Ca^{2+} (Biological Industries). Thereafter, the EBs were transferred into a dissociation solution containing (mM): 120 NaCl, 5.4 KCl, 5 $MgSO_4$, 5 Na-pyruvate, 20 glucose 20 taurine, 10 4-(L-Hydroxyethyl) piperazine-1-ethanesulfonic acid (HEPES) at pH 6.9 and 30 μM $CaCl_2$ supplemented with 1 mg/ml collagenase B (Roche, Basel, Switzerland) at 37°C for 30 min. After a brief centrifuge (1 min., 800 rpm), the cells were incubated for 15 min. in 'KB medium' solution containing (mM): 85 KCl, 30 K_2HPO_4, 5 $MgSO_4$, 1 EGTA, 2 Na_2ATP, 5 Na-pyruvate, 5 creatine, 20 taurine and 20 glucose, at pH 7.2, 37°C.

Analysis of mRNA expression by RT-PCR

Total RNA was isolated using TRIzol Reagent (Invitrogen, Carlsbad, CA, USA) from undifferentiated ES and iPS cells, and from contracting areas micro-dissected from 30–40-day-old EBs. Total RNA (1 μg) was used for cDNA synthesis with SuperScript™ II Reverse Transcriptase (Invitrogen). One microlitre of cDNA was amplified by PCR with BioTaq DNA-polymerase (Bioclone, Taunton, MA, USA) in Taq ×10 reaction buffer, with the use of 0.5 μl of each primer and 0.5 μl dNTPs (1 mM) in a 10 μl reaction. Controls without reverse transcriptase excluded false-positive results due to contamination with genomic DNA. PCR primers used in this study: Tbx-5: F: TACCACCACACCCATCAAC, R: ACACCAAGACAGGGACAGAC, 62°C; Tbx20: F: CTGAGCCACTGATCCCCACCAC, R: CTCAGGATCCACCCCCGAAAAG,

© 2011 The Author

Journal of Cellular and Molecular Medicine © 2011 Foundation for Cellular and Molecular Medicine/Blackwell Publishing Ltd

72°C; α-cardiac actin: F: GGAGTTATGGTGGGTATGGGTC, R: AGTGGTGACAAAGGAGTAGCCA, 65°C; C-Troponin: F: GGCAGCGGAAGAGGATGCTGAA, R: GAGGCACCAAGTTGGGCATGAACGA, 66°C; glyceraldehyde-3-phosphate dehydrogenase (GAPDH): F: AGCCACATCGCTCAGACACC, R: GTACTCAGCGGCCAGCATCG, 60°C; Oct4: F: TTCTGGCGCCGGTTACAGAA, R: GAGAACAATGAGAACCTTCAGG, 55°C; Sox2: F: CTGTCATTTGCTGTG, R: GGGAGGGGTGCAAA, 68°C; Nanog: F: TGAGTGTGGATCCA, R: TGAATAAGCAGATC, 63°C; Rex1: F: ACAGTCCAGCAGGT, R: CTTGTCTTTGCCCGT, 63°C; c-myc F: ACTCTGAGGAGGAACAAG, R: TGGAGACGTGGCACCTCTT, 58°C; Klf4: F: CTCAAGGCACACCTG, R: AGTGCCTGGTCAGTT, 60°C.

Immunofluorescence staining

Micro-dissected contracting areas from 25–60-day-old EBs were plated on cover slips coated with 0.1% gelatine solution or with fibronectin, and stained to detect characteristic cardiomyocyte proteins. Alternatively, the contracting areas were dissected and dissociated to obtain small clusters of contracting cardiomyocytes. Thereafter, the cells were fixed in 4% paraformaldehyde for 15 min. at room temperature, rinsed three times in PBS and permeabilized in 0.5% Triton X-100 (Sigma-Aldrich) diluted in PBS for 10 min. Samples were blocked with 2% goat serum in 0.5% Triton X-100 for 10 min. at room temperature. The following primary antibodies were used: rabbit monoclonal IgG1 anti-cardiac troponin I antibody (1:400; clone EP1106Y, Abcam, Cambridge, UK), mouse monoclonal IgG1 anti-sarcomeric α-actinin antibody (1:600; clone EA-53, Sigma-Aldrich), mouse monoclonal IgG1 anti-myosin heavy chain antibody (1:50; clone SMMS-1, Dako, Glostrup, Denmark), mouse monoclonal IgG2b anti-troponin I (1:2000, Chemicon, Temecula, CA, USA), polyclonal rabbit anti-calsequestrin 2 (H-60) antibody (1:75, Santa Cruz, Santa Cruz, CA, USA) or polyclonal rabbit anti-ryanodine receptor 2 (1:1000, Chemicon). The cells were incubated for 1 hr at room temperature or overnight at 4°C with the primary antibody diluted in blocking solution, and then rinsed three times for 5 min. with PBS. Further incubation was performed with the appropriate secondary antibody for 30 or 60 min. at room temperature: Cy3-conjugated donkey antimouse IgG (1:200; Sigma-Aldrich), Alexa Fluor® 488 donkey anti-rabbit IgG (1:100; Invitrogen), Cy3-conjugated goat anti-rabbit IgG (1:50, Jackson Immunoresearch, West Grove, PA, USA) or Cy2-conjugated goat antimouse IgG (1:50, Jackson Immunoresearch), each diluted in a blocking solution. The cells were rinsed once more, counterstained with 4′, 6′-diamidino-2-phenylindole (DAPI) (Sigma-Aldrich), and analysed with LSM 510 Meta laser scanning confocal system (Zeiss, Oberkochen, Germany). For pluripotent analysis the following primary antibodies were used: polyclonal rabbit anti-Oct4 (1:50, Santa Cruz) monoclonal mouse anti-stage specific embryonic antigen (SSEA)4 (1:50, MC-813, DSHB, Iowa city, IA, USA) monoclonal mouse anti-tumour recognition antigen (TRA)-1–60 (1:50, Chemicon) and monoclonal mouse anti-TRA-1–81 (1:50, Chemicon). For EBs differentiation to the three germ layer derivatives analysis, dissociated EBs were re-plated onto gelatine covered plates and grown for 14 days. The following primary antibodies were used: polyclonal rabbit anti-α Fetaprotein (Dako), mouse monoclonal anti-smooth muscle actin (SMA) antibody (1:50, Dako), polyclonal rabbit anti-β-tubulin III (1:1000, Covance, Princeton, NJ, USA) and monoclonal mouse anti-Nestin (1:200, Chemicon).

Teratoma formation and immunohistochemical staining

For teratoma generation, 2×10^6 cells were injected into the flanks of recipient severe combined immunodeficient (SCID) mice. Teratomas were isolated for histological analysis 6–8 weeks later, embedded in paraffin and sectioned. Paraffin sections were deparaffinized by Xylol/Xylene then rehydrated with propanol and washed with distilled water. Sections were stained with haematoxylin and eosin according to standard protocols. Imunnofluorescence staining was performed as described above.

Measurements of $[Ca^{2+}]_i$ transients and contractions

$[Ca^{2+}]_i$ transients and contractions were measured from small contracting areas of EBs or from dissociated EBs by means of fura-2 fluorescence and video edge detector, respectively [15, 16]. Briefly, spontaneously contracting areas were mechanically dissected, and adhered onto 30-mm-diameter fibronectin coated glass slides. Subsequently, fura 2-stained contracting areas were transferred to a chamber mounted on the stage of an inverted microscope and perfused with Tyrode's solution [15] at 37°C. The preparations were stimulated at a frequency 10% higher than the spontaneous rate; in the majority of experiments, a stimulation frequency of 0.5–1 Hz was sufficient to override the spontaneous beating rate. The acquisition rate of both the $[Ca^{2+}]_i$ transients and contractions was 100 points/sec. To characterize the contraction amplitude, the differences between minimal and maximal video cursor positions (L_{Amp}) were calculated in 10 successive contractions and averaged. The maximal rates of contraction ($dL/dt_{Contrac}$) and relaxation (dL/dt_{Relax}) were calculated and averaged over 10 contractions. Specifically, $dL/dt_{Contrac}$ is the maximum derivative of the line that represents the cell movement during the contraction (measured with the edge detector). dL/dt_{Relax} is the maximum derivative of the line that represents the cell movement during relaxation.

The micro-electrode-array data acquisition system

Unipolar electrograms were recorded from iPS-CM plated on micro-electrode arrays (MEAs) (Multi Channel Systems, Reutlingen, Germany) as previously described [17, 18]. In brief, the MEA plate contains 8×8 matrix of 60 titanium–nitride, 30-μm-diameter electrodes, embedded in its centre, with an inter-electrode distance of 200 μm. For the electrophysiological measurements, MEAs were removed from the incubator, placed in the recording apparatus preheated to 37°C. Spontaneous electrical activity of the iPS-CM was recorded within 5 min. after removal from the incubator. The electrogram analysis was performed automatically using custom-made MATLAB (MATLAB® 6.5) routines. The local activation times (LAT) at each electrode, defined as the time of occurrence of the first derivative plot minimum of the fast activation phase, was used to construct activation maps and calculate conduction velocity. The scalar value of local conduction velocity was calculated at each of the array electrodes as previously described [17, 18]. Finally, the conduction velocity shown for each measurement is the average of all the local velocities calculated at each of the 60 recording electrodes.

Chemicals

Unless otherwise indicated, chemicals were purchased from Sigma (Sigma-Aldrich Israel, Rehovot, Israel).

Statistical analysis

Results were expressed as mean ± S.E.M. Means of two populations were compared using Student's t-test for paired observations. Two-way ANOVA

© 2011 The Author
Journal of Cellular and Molecular Medicine © 2011 Foundation for Cellular and Molecular Medicine/Blackwell Publishing Ltd

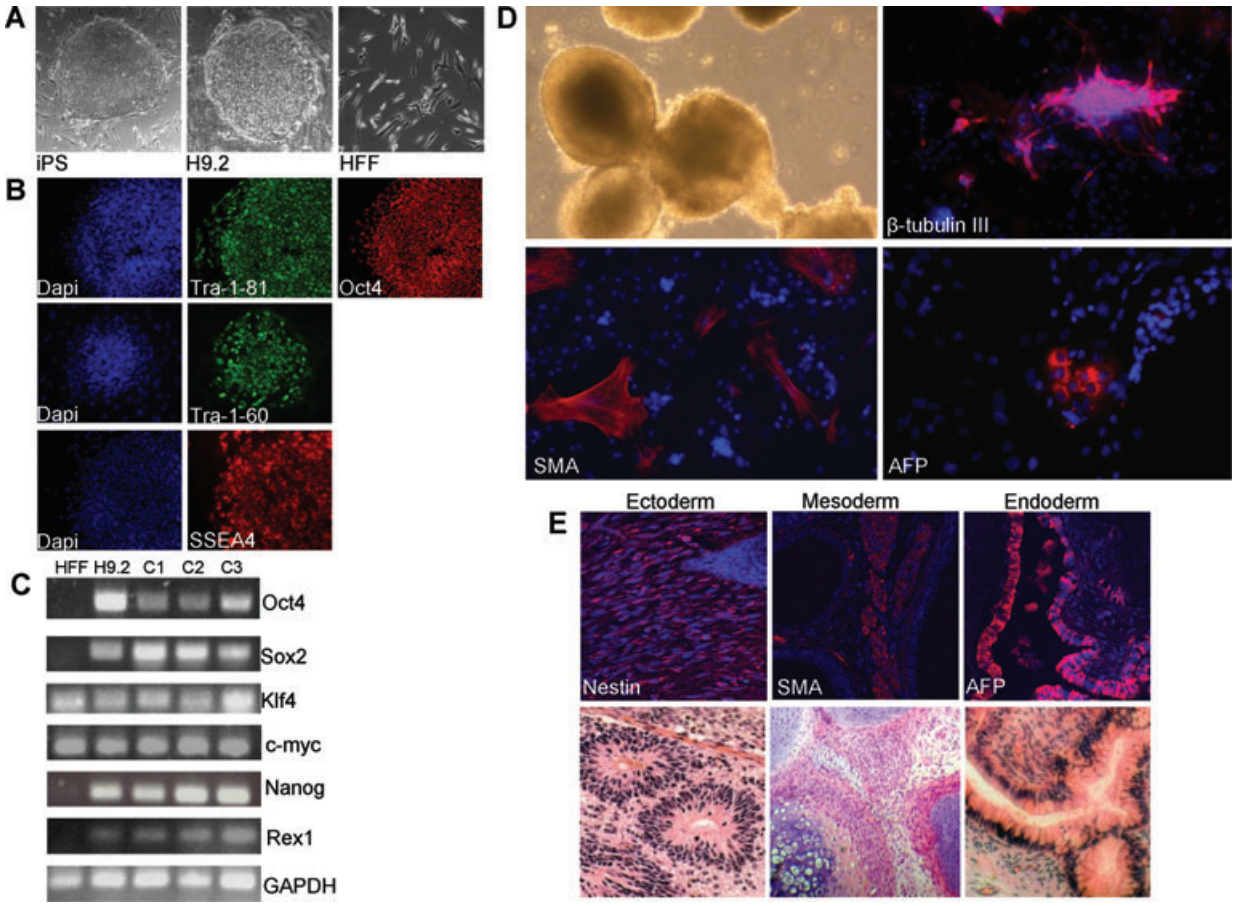

Fig. 1 iPS characterization as pluripotent ES-like cells: Human iPS were derived from HFF cells following retroviral infection with the four reprogramming factors and display morphology similar to that of hES cells: (**A**) iPS colony, hES (H9.2) colony and HFF morphology. (**B**) Immunofluorescence staining for pluripotent markers: Oct4, TRA-1–81, TRA-1–60 and SSEA4 for iPS clone 3. DAPI nuclear staining indicated on left panel. (**C**) Analysis of gene expression by PCR. The transcription of Oct4, Sox2, c-myc, Klf4, Nanog and Rex1 were analysed in three iPS clones C1, C2 and C3 as well in the hESC clone–H9.2 and parental HFF. GAPDH was used as amplification and loading control. (**D**, **E**) Spontaneous differentiation of human iPS into EBs and teratomas. Human iPS were induced to spontaneous differentiation *in vitro* and *in vivo*. (**D**) The upper left panel illustrates EBs derived from human iPS clone 3. Upper right and bottom left and right panels show immunofluorescence staining for markers of the three germ layers in human IPS derived EBs. Representative ectoderm marker β-tubulin-III, representative mesoderm marker SMA and representative endoderm marker α-Fetoprotein (**E**) Immunofluorescence staining for different markers (up) and haematoxylin and eosin staining demonstration of typical tissue morphology (bottom) were performed on teratomas to confirm derivatives of the three germ layers: ectoderm – representative marker Nestin staining and neural rosettes, mesoderm – SMA marker staining and cartilage endoderm – α-Fetoprotein marker staining and gut like epithelium.

test was performed followed by Bonferroni t-test for all pairwise multiple comparison procedures, using SigmaStat 3.11 software (Aspire Software International, Ashburn, VA, USA). A value of $P < 0.05$ was considered significantly different.

Results

Generation of iPS cells

The HFF cells infected with the supernatant mix of the four retroviruses expressing the human reprogramming transgenes – Oct4, Sox2, Klf4 and c-Myc, were grown in MEF-conditioned medium. Approximately 24 days after infection, some iPS colonies morphologically resembling hESC emerged (Fig. 1A). Three clones were selected, propagated and grown for over 50 passages. The karyotype of the iPS was examined and verified for no chromosomal abnormalities. To examine the three clones for ES-like properties, expression of the hESC surface antigens TRA-1–81, TRA-1–60, SSEA-4 and the pluripotent marker Oct4 was tested by immunofluorescence (Fig. 1B) and hESC immunofluorescence signature gene expression was tested by RT-PCR (Fig. 1C).To ensure that these ESC-like colonies are capable of differentiating, they were spontaneously differentiated into EBs. The EBs were

© 2011 The Author

Journal of Cellular and Molecular Medicine © 2011 Foundation for Cellular and Molecular Medicine/Blackwell Publishing Ltd

analysed for the presence of cells differentiating into the three germ layers: endoderm, mesoderm and ectoderm, using well-established biomarkers (Fig. 1D). The EBs were further differentiated into contracting cardiac clusters. To confirm the true pluripotent nature of iPS cells, we formed teratomas by injecting iPS cells into SCID mouse and verified differentiation into the three germ layers by immunohystochemistry and haematoxylin and eosin staining (Fig. 1E). Overall, these iPS exhibit true hESC-like properties, as demonstrated by their pluripotent gene expression and capability of differentiating into derivatives of the three germ layers.

Molecular characterization of iPS-CM

To characterize the differentiation of undifferentiated human iPS cells into functional cardiomyocytes, we investigated in undifferentiated cells and in micro-dissected contracting regions from EBs, the expression pattern of several key genes in cardiac muscle differentiation using RT-PCR. Both iPS cells and ES cells were analysed and compared (Fig. 2A). T-box 5 (Tbx5) and T-box 20 (Tbx20) were included as markers for cardiac mesoderm; the myofilament protein genes cardiac troponin T and α-cardiac actin served as markers for cardiomyocytes. Controls without reverse transcriptase were used to exclude false-positive results based on contamination with genomic DNA.

The RT-PCR analysis (Fig. 2A) demonstrates that although mesodermal and cardiac markers were detectable in undifferentiated iPS and ES cell cultures, a strong increase in their expression was evident in contracting EBs, with a similar expression pattern for both iPS and ES-derived cells. These results are similar to those reported for both mouse and human iPS-CM [11–12, 19].

To further characterize iPS-CM, immunofluorescence staining was performed on micro-dissected contracting areas, and on cardiomyocytes dissociated thereof. As illustrated in Fig. 2B, the cells were positive for α-sarcomeric actinin, cardiac troponin I and myosin heavy chain, and exhibited areas of cross-striations Importantly, an overlap was found between the fluorescence signal of cardiac troponin, which is a highly cardiac-specific myofilament protein, and each of the other proteins. The positive immunostaining of multiple myofilament proteins suggests that a preliminary organization of a sarcomeric structure can develop in iPS-CM, similarly to ES-derived cardiomyocytes, resembling previous reports on cardiomyocytes derived from other mouse and human iPS clones [11–12, 19].

$[Ca^{2+}]_i$ transients and contractions in iPS-CM

To investigate (see subsequent sections) the basic properties of the $[Ca^{2+}]_i$ handling machinery and mechanical function, $[Ca^{2+}]_i$ transients and contractions were recorded from small contracting clusters of iPS-CM by means of fura-2 fluorescent and video edge detector, respectively. As illustrated in Fig. 3A–C, the representative traces of $[Ca^{2+}]_i$ transients and contractions from the iPS-CM clones C1 and C2 (stimulated at 0.5 Hz) are similar to those recorded from hESC-derived cardiomyocytes (hESC-CM) [15] as well as from a variety of cardiac preparations. Hence, these findings indicate that iPS-CM exhibit 'cardiac-like' features of the excitation–contraction coupling machinery.

The inotropic responsiveness of iPS-CM to β-adrenergic stimulation

In order to determine whether iPS-CM are responsive to β-adrenergic stimulation, we generated concentration-response relations of the effect of isoproterenol on the contraction parameters. In support of the functionality of the β-adrenergic signalling pathway, isoproterenol caused (within 2–3 min.) a marked concentration-dependent positive inotropic effect (Fig. 3D). To establish whether the inotropic response is developmentally regulated, we analysed the effect of isoproterenol on the contraction parameters in two age groups: 10–15- and 18–70-day-old iPS-CM. As seen in Fig. 3E, in both age groups isoproterenol caused a significant ($P < 0.05$) increase in the maximal rates of contraction and relaxation, and in the contraction amplitude. Although for all three contraction parameters, the older group appears more responsive, only for the maximal rate of contraction (dL/dt_{max}) the difference was statistically different ($P < 0.05$). In view of these findings, in future studies we will explore the mechanisms underlying the developmental changes in the β-adrenergic responsiveness.

Recording extracellular electrograms from iPS-CM

Unipolar electrograms were recorded from iPS-CM plated on MEAs as previously described [17, 18]. In order to generate meaningful activation maps, for these experiments we selected large and flat spontaneously contracting EBs which covered most of the recording electrodes. Indeed, as seen in Fig. 4A, extracellular electrograms (an expansion of the electrogram recorded at electrode #66 is shown in Fig. 4B) were readily recorded in most of the MEA electrodes. By calculating the LAT at each electrode, we generated an activation map (Fig. 4C), which demonstrated that activation propagated from the bottom right corner to the upper left corner, at an average conduction velocity of 9.25 cm/sec. In summary, in three EBs, conduction velocity, the maximal upstroke velocity of activation (dV/dt_{max}) and 'QRS' duration were (mean $\pm$ S.E.M.): 10.38 $\pm$ 2.38 cm/sec., 1.03 $\pm$ 0.24 μV/sec. and 1.53 + 0.26 msec.

Force frequency relations

A fundamental property of the adult human myocardium is its ability to increase the contraction force in response to increased rate of stimulation. The phenomenon termed positive force–frequency

© 2011 The Author
Journal of Cellular and Molecular Medicine © 2011 Foundation for Cellular and Molecular Medicine/Blackwell Publishing Ltd

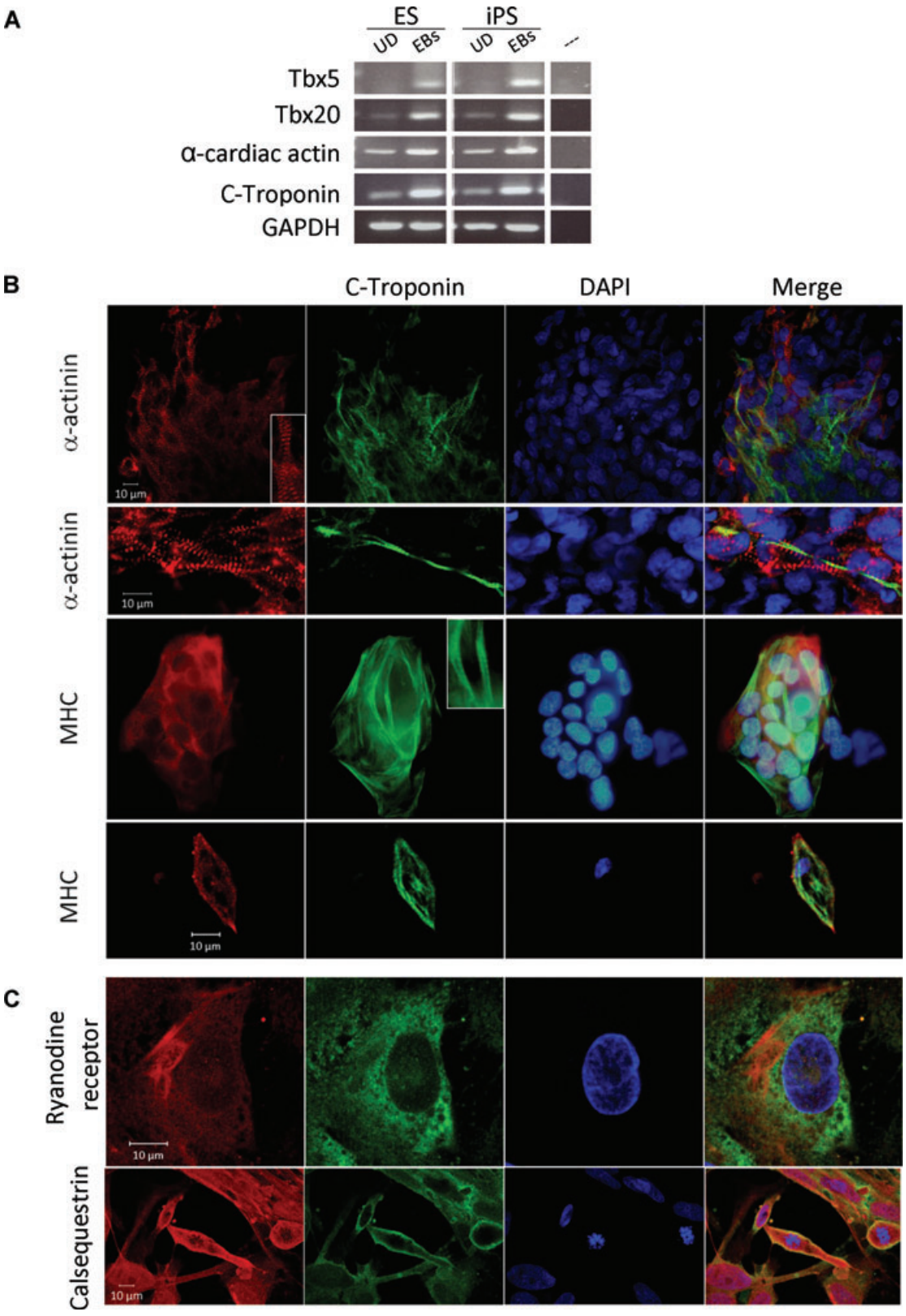

© 2011 The Author

Journal of Cellular and Molecular Medicine © 2011 Foundation for Cellular and Molecular Medicine/Blackwell Publishing Ltd

Fig. 2 Molecular characterization of iPS-derived cardiomyocytes. (**A**) RT-PCR analysis of cardiac markers in iPS-derived cardiomyocytes clone C2. Undifferentiated cells and micro-dissected contracting areas from EBs, from both iPS and ES cells were analysed for their expression of cardiac mesoderm (T-box 5 [Tbx5] and T-box 20 [Tbx20]) and cardiac markers (cardiac troponin T and α-cardiac actin). To exclude false-positive results due to contamination with genomic DNA, adequate controls without RT (–) were used. (**B**) Immunofluorescence staining of cardiac proteins in iPS-derived cardiomyocytes clone C2. Micro-dissected contracting areas from iPS-derived cardiomyocytes or cells clusters dissociated from these areas were stained for typical myofilament proteins. Cells were co-labelled with anti-cardiac troponin I (green) and either anti-sarcomeric α-actinin or myosin heavy chain (red). Nuclei were stained with DAPI (blue). Representative areas with apparent cross-striations are focused in the inserts. (**C**) Immunofluorescence staining of ryanodine receptor and calsequestrin in iPS-derived cardiomyocytes clone C2. Spontaneously contracting iPS-derived cardiomyocytes were fixed and stained as described in 'Methods' section. Red staining is for ryanodine receptor or calsequestrin; green staining is for the cardiac marker troponin I; blue staining is DAPI nuclei, and the last panel is a merge of all three layers. Magnification for ryanodine receptor staining is 2.7 $\times$ 63. Magnification for calsequestrin staining is 1 $\times$ 63.

relations (FFRs), which is related to SR Ca^{2+} release, is utilized by the heart to increase cardiac output under exercise or stress conditions. To generate FFRs, iPS-CM preparations were stimulated at increasing frequencies (0.5, 0.7, 0.9, 1 and 1.2 Hz), and contraction was measured at each frequency after steady state was attained. Although we used high voltages and long stimulus durations, we were unable to stimulate the EBs above at stimulation rates >1.2–1.5 Hz. As depicted by the representative experiments, both in the iPS-CM clones investigated and in the hESC-CM clone H9.2 investigated, increasing the rate of stimulation caused a decrease in contraction amplitude (Fig. 5A–D). Please note that the discontinuous traces in Fig. 5A–D result from digitalization of the original signal which was sampled at 100 points/sec. In summary, both iPS-CM clones and the hESC-CM clone H9.2 exhibited the same extent of negative FFRs, which was statistically significant ($P < 0.05$, two-way ANOVA) for all the clones investigated (Fig. 5E).

Post-rest potentiation in iPS-CM

Post-rest potentiation (PRP) is a mechanical phenomenon dependent on SR Ca^{2+} release, which in the adult heart is manifested by the fact that a post-rest contraction is stronger than the pre-rest (control) contraction. To test the presence of PRP in iPS-CM, the basic stimulation rate of 0.5 Hz was interrupted by pauses of varying lengths (5, 10, 30 and 60 sec.), followed by resumption of the regular stimulation protocol for 60 sec. Thus, PRP is defined as the ratio between the first post-rest contraction and the pre-rest contraction. Figure 6A and B depicts two representative experiments illustrating that mild PRP is present (although to a different extent) in both clones. Figure 6C depicts a representative experiment illustrating no PRP in hESC-CM in agreement with our previous findings [15]. The summary of these experiments demonstrates that while iPS-CM clone C2 present 10–15% degree of potentiation (post-rest/pre-rest contraction amplitude) or up to nearly 40% degree of potentiation in the case of iPS-CM clone C1, hESC-CM present practically no potentiation ($P < 0.05$, two-way ANOVA). The dependency on the rest interval was not statistically significant for either of the cell types investigated (Fig. 6D). Importantly, pause periods in which spontaneous contractions interrupted the pause were not included in the analysis (*i.e.* 90-sec. pauses). In agreement with previous reports [*e.g.* 20], more prominent PRP was also observed when the basic stimulation frequency was increased to 1 Hz in both iPS-CM clones investigated (data not shown).

Does SR Ca^{2+} release contribute to contraction in iPS-CM?

A key aspect of the excitation–contraction coupling machinery is Ca^{2+}-induced Ca^{2+} release from the SR, which provides (in most mature hearts) the majority of Ca^{2+} ions utilized by the contractile machinery [21]. To further evaluate the SR function in iPS-CM, we investigated the effects of ryanodine and caffeine on the contractions and $[Ca^{2+}]_i$ transients. Importantly, these experiments were performed on dissociated EBs with a diameter range of 0.3–0.7 mm (see the 'Methods' section for the dissociation protocol). Firstly, we determined the effect of ryanodine (10 μM), which at this 'blocking' concentration, causes a prominent negative inotropic effect [22, 23]. As depicted by a representative experiment (Fig. 7A) in a 60-day-old EB, ryanodine caused a prominent negative inotropic effect which was partially reversible, supporting the notion of a functional SR. Since in our recent study [15] we showed that ryanodine does not affect hESC-CM contraction recorded from intact EBs, in order to be compatible with the present work, we repeated these experiments in dissociated hESC-derived EBs. As depicted by a representative experiment (Fig. 7B) in a 30-day-old hESC-CM clone H9.2 and in agreement with our previous work, ryanodine did not affect the contraction of dissociated hESC-derived EBs (Fig. 7B). As shown by the summary (Fig. 7C), while in both iPS-CM clones C1 and C2 (four to seven experiments) ryanodine decreased significantly ($P < 0.05$) all three contraction parameters, in hESC-CM clone H9.2 (four experiments) ryanodine did not exert any negative effect. Next, we tested the response of iPS-CM clones C1 and C2 to a brief exposure to caffeine (10 mM), which commonly causes an abrupt SR Ca^{2+} release in a variety of cardiac preparations [24, 25]. As shown in 10-day-old iPS-CM from clone 2 (Fig. 7D), and in the summary of four experiments (Fig. 7E), caffeine (10 mM) caused a small ($P < 0.05$) increase in diastolic $[Ca^{2+}]_i$. A similar response

© 2011 The Author
Journal of Cellular and Molecular Medicine © 2011 Foundation for Cellular and Molecular Medicine/Blackwell Publishing Ltd

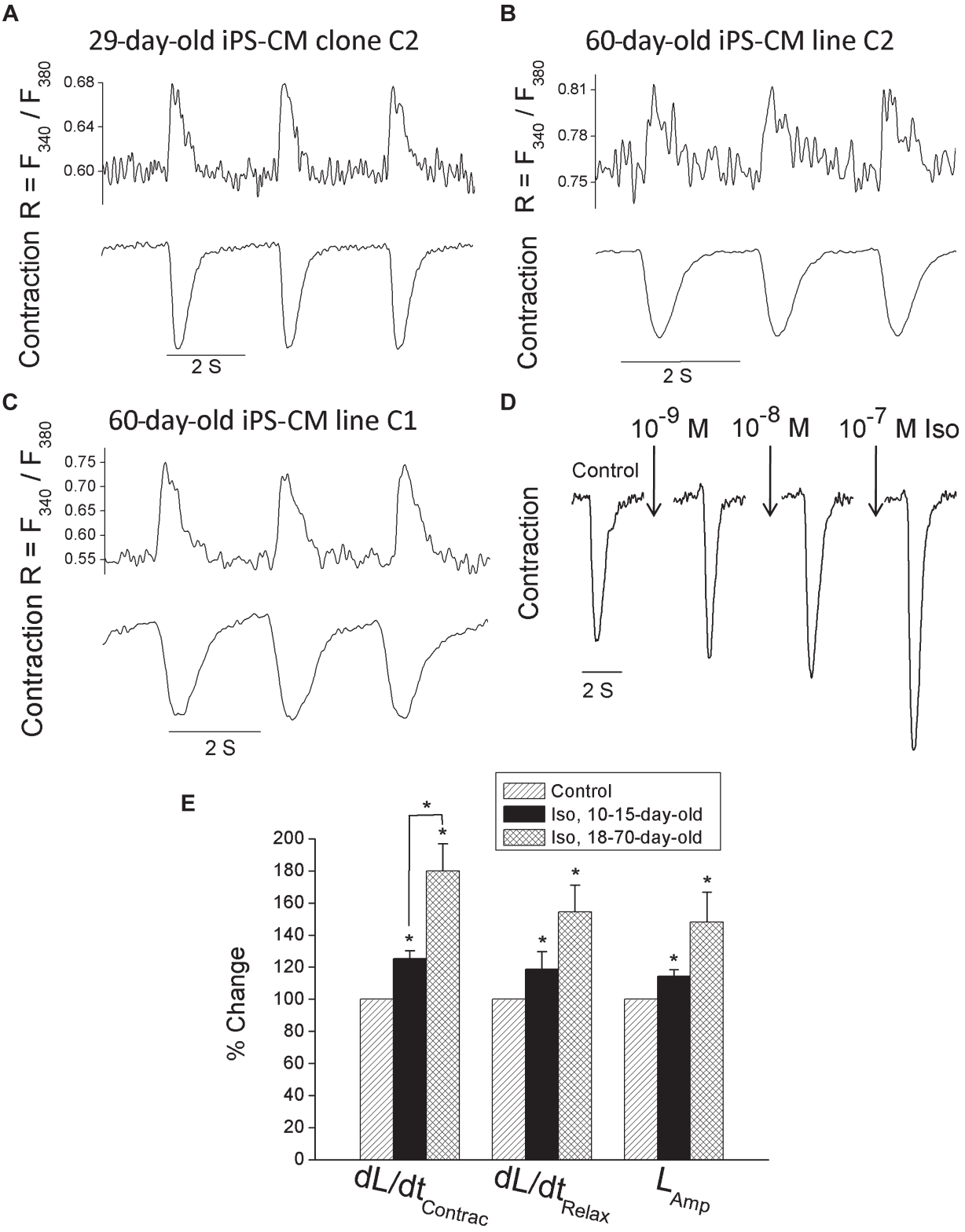

© 2011 The Author
Journal of Cellular and Molecular Medicine © 2011 Foundation for Cellular and Molecular Medicine/Blackwell Publishing Ltd

Fig. 3 Simultaneous recordings of $[Ca^{2+}]i$ transients and contractions of spontaneously contracting clones C1 and C2 iPS-derived cardiomyocytes and the effect of isoproterenol on iPS-derived cardiomyocytes clone C2. (**A**–**C**) Simultaneous recordings of $[Ca^{2+}]i$ transients and the contraction in 29- and 60-day-old clone C2 iPS-derived cardiomyocytes (**A**, **B**) and a 60-day-old clone C1 iPS-derived cardiomyocytes (**C**). (**D**) A representative experiment illustrating an increase in contraction amplitude in response to increasing concentrations of isoproterenol (the preparation was 18-day-old and stimulated at 0.5 Hz). (**E**) A summary of the effects of isoproterenol on the contraction parameters of 10–15- and 18–70-day-old iPS-derived cardiomyocytes clone C2 ($n = 5$ and $n = 5$–6, respectively). The effects of isoproterenol are presented as maximal responses (regardless of the drug concentration) and presented as percentage change of their respective controls. $*P < 0.05$. Abbreviations: iPS-CM, induced pluripotent stem cell-derived cardiomyocytes; Iso, isoproterenol; $dL/dt_{Contrac}$, maximal rate of contraction; dL/dt_{Relax}, maximal rate of relaxation; L_{Amp}, contraction amplitude.

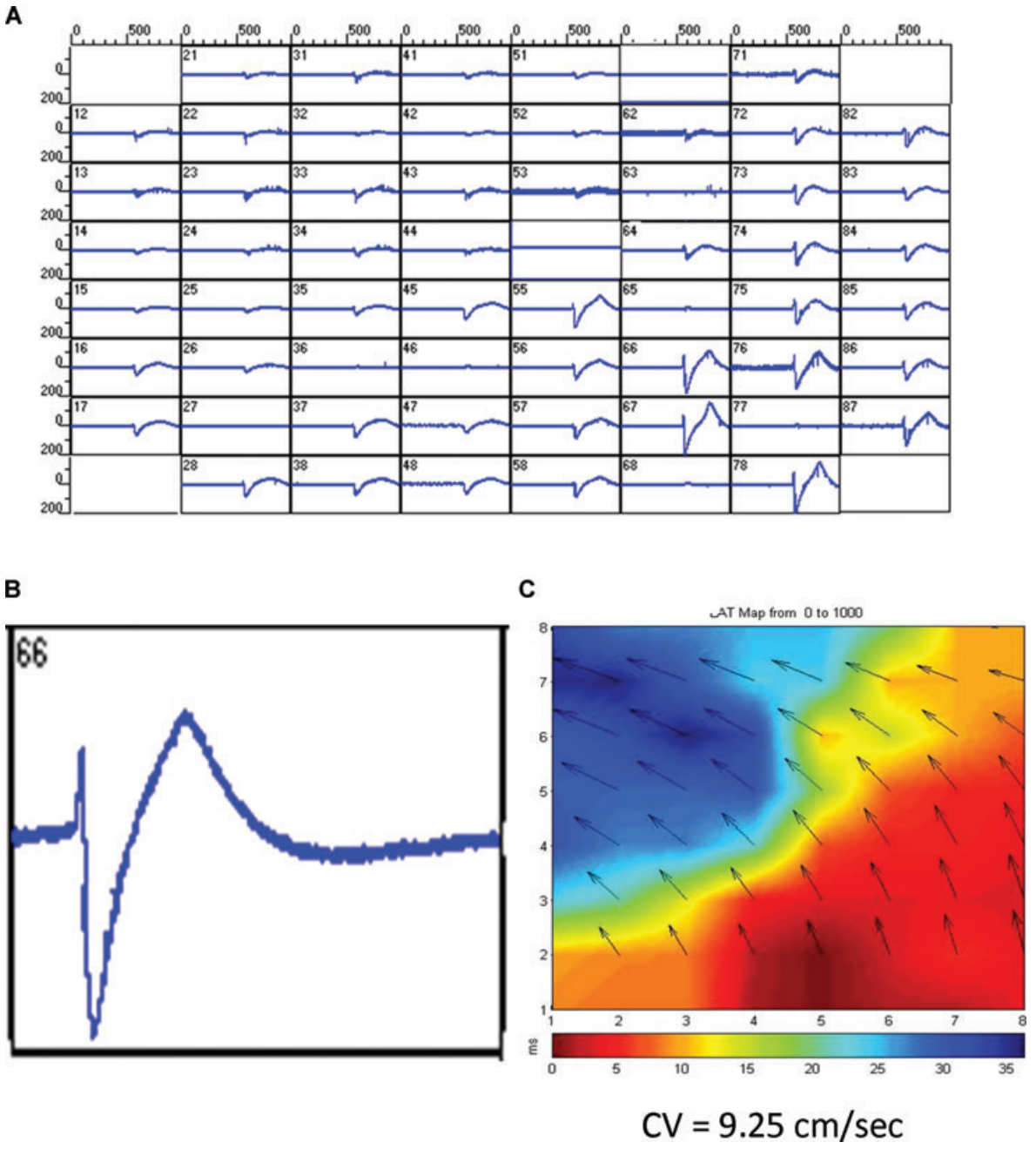

© 2011 The Author
Journal of Cellular and Molecular Medicine © 2011 Foundation for Cellular and Molecular Medicine/Blackwell Publishing Ltd

Fig. 4 Extracellular electrograms and an activation map in a network of iPS-derived cardiomyocytes recorded by means of the MEA data acquisition system. (**A**) A representative display of electrograms recorded from the entire MEA array. (**B**) A representative electrogram recorded at electrode # 66. (**C**) An activation map serving as a visual representation of the activation sequence. The map activation time (the time duration between first and last activations) is represented by the lower scale at the bottom of the map. The colour strip below the map represents the colour spectrum and its scaling according to time. Colour coding: red – early; blue – late.

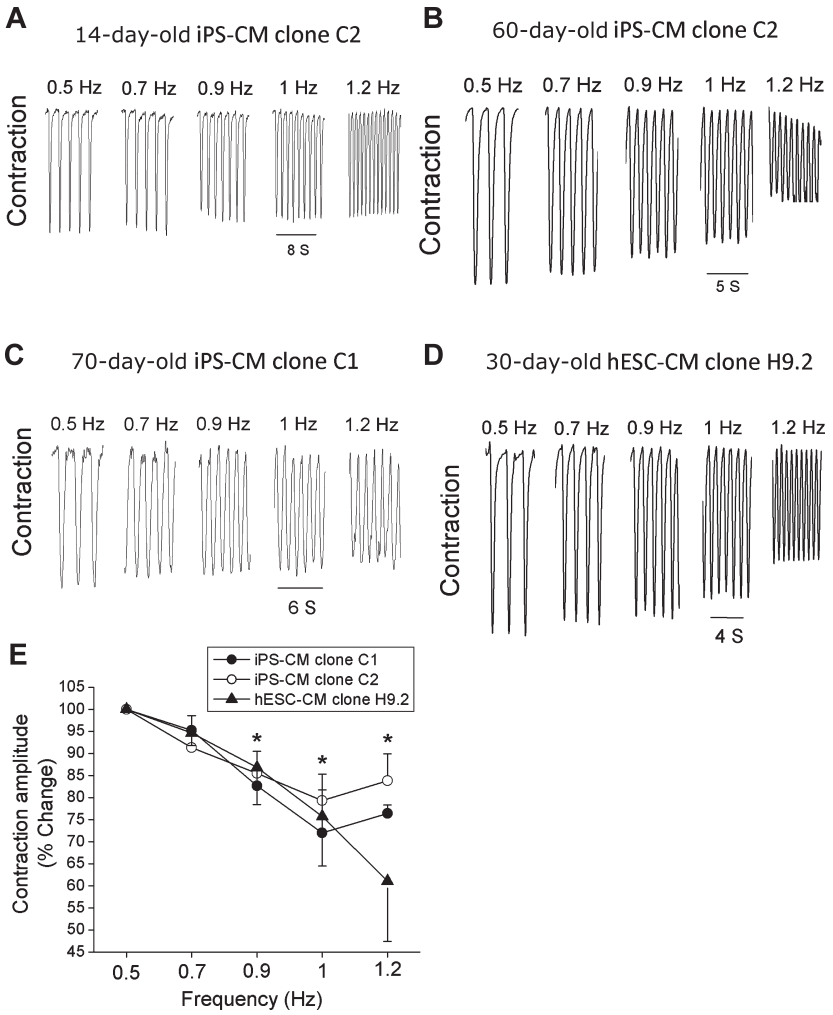

Fig. 5 FFRs in iPS-derived cardiomyocytes clones C1 and C2 and in hESC-derived cardiomyocytes clone H9.2. (**A**–**D**) Representative experiments illustrating a decrease in contraction amplitude in response to increase stimulation frequency in 14- (**A**) and 60-day-old (**B**) iPS-derived cardiomyocytes clone C2, in 70-day-old (**C**) iPS-derived cardiomyocytes clone C1 and in 30-day-old (**D**) hESC-derived cardiomyocytes clone H9.2. To generate the FFRs, contracting EBs were paced by means of electric field stimulation at 0.5, 0.7, 0.9, 1 and 1.2 Hz. (**E**) Average percentage change in contraction amplitude in response to increase in stimulation frequency in iPS-derived cardiomyocytes clone C2 ($n = 7$), clone C1 ($n = 6$) and in hESC-derived cardiomyocytes clone H9.2 ($n = 3$). The results are expressed as percentage change from the values at 0.5 Hz. $^*P < 0.05$.

to caffeine was also obtained in iPS-CM from clone C1 (data not shown). Collectively, these results show that while in iPS-CM (clones C1 and C2) caffeine causes a much smaller response than in adult cardiomyocytes, caffeine-induced SR Ca^{2+} release is measurable.

Finally, to further establish the SR Ca^{2+}-release machinery in iPS-CM, we determined the immunofluorescence expression of the ryanodine receptor and calsequestrin, both key elements of SR function. Indeed, as demonstrated in Fig. 2B, troponin I positive cells (*i.e.* cardiomyocytes) were clearly positive for ryanodine (30-day-old iPS-CM clone C2) and calsequestrin (45-day-old iPS-CM clone C2). Similar findings for ryanodine were repeated in four EBs clone C2, and for calsequestrin in three EBs clone C2.

Discussion

The present study is the first report on the functional properties related to $[Ca^{2+}]_i$ handling and contraction, the contribution of SR Ca^{2+} release to contraction and the β-adrenergic inotropic responsiveness, in iPS-CM. Our major findings show that iPS-CM: (1) express cardiac specific RNA and proteins; (2) exhibit negative

© 2011 The Author

Journal of Cellular and Molecular Medicine © 2011 Foundation for Cellular and Molecular Medicine/Blackwell Publishing Ltd

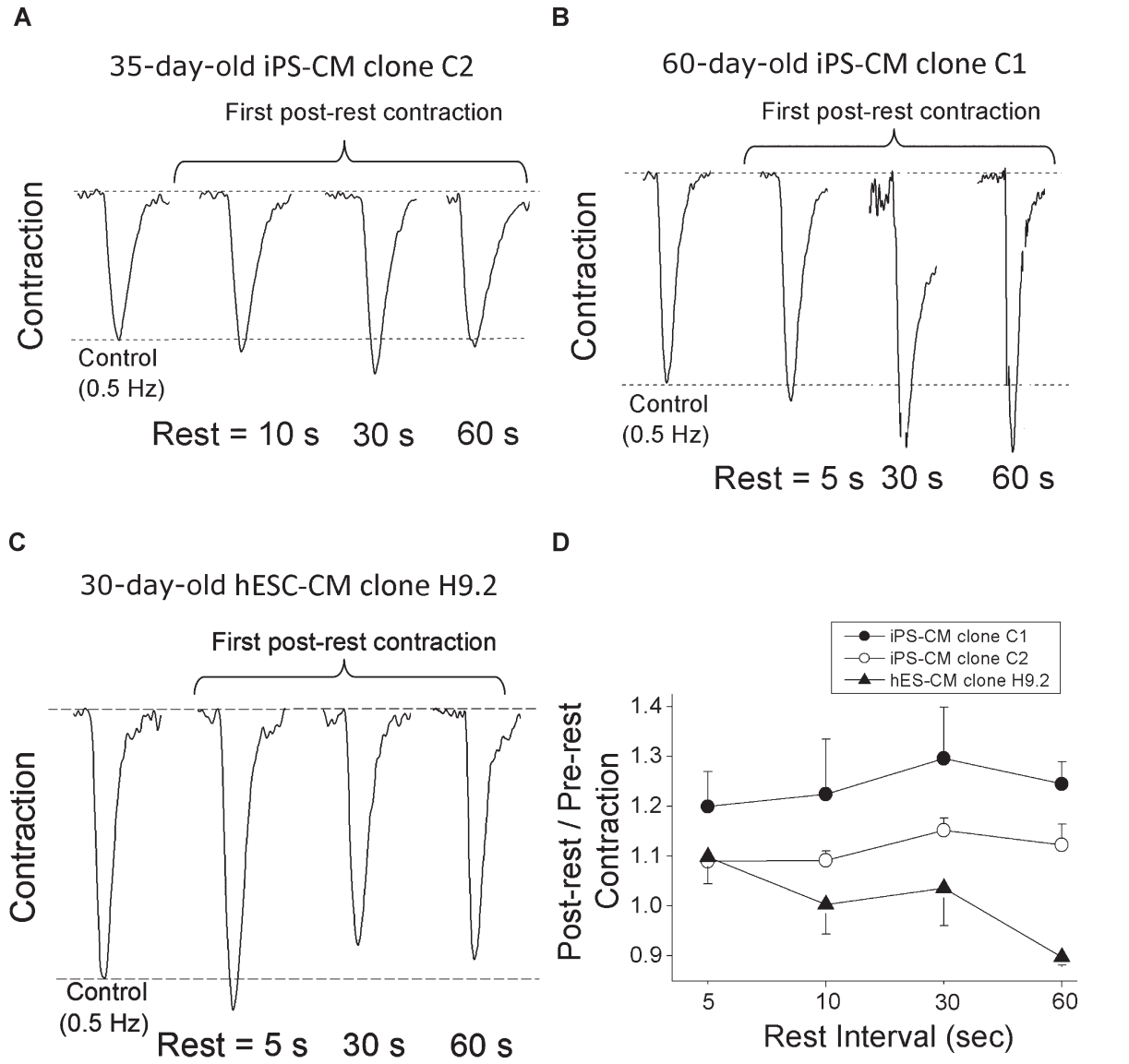

Fig. 6 PRP in iPS-derived cardiomyocytes clones C1 and C2 and in hESC-derived cardiomyocytes clone H9.2. (**A**) Representative PRP contraction tracings from 35-day-old iPS-derived cardiomyocytes clone C2, depicting the control contraction recorded at 0.5 Hz, and the first post-rest contractions after rest periods of 10, 30 and 60 sec. (**B**) Representative PRP contraction tracings from 60-day-old iPS-derived cardiomyocytes clone C1, depicting the control contraction recorded at 0.5 Hz, and the first post-rest contractions after rest periods of 5, 30 and 60 sec. (**C**) Representative PRP contraction tracings from 30-day-old hESC-derived cardiomyocytes clone H9.2, depicting the control contraction recorded at 0.5 Hz, and the first post-rest contractions after rest periods of 5, 30 and 60 sec. (**D**) Average post-rest/pre-rest contraction amplitude ratios in 0.5 Hz paced iPS-derived cardiomyocytes clones C2 ($n = 7$) and clone C1 ($n = 3$) and in hESC-derived cardiomyocytes clone H9.2 ($n = 3$).

FFRs and positive PRP; (3) respond to ryanodine and caffeine, and express the SR-Ca^{2+} handling proteins ryanodine receptor and calsequestrin. Hence, this study demonstrates that in cardiomyocytes differentiated from HFF-derived iPS, the functional properties related to excitation–contraction coupling, resemble in part those of adult cardiomyocytes.

Molecular characterization of ES-like iPS colonies and iPS-CM

In agreement with previous reports [10, 11] we confirmed that our iPS clones represent ESC-like pluripotent cells by demonstrating that the colonies: (1) resemble in their morphology hESC (Fig. 1A);

© 2011 The Author
Journal of Cellular and Molecular Medicine © 2011 Foundation for Cellular and Molecular Medicine/Blackwell Publishing Ltd

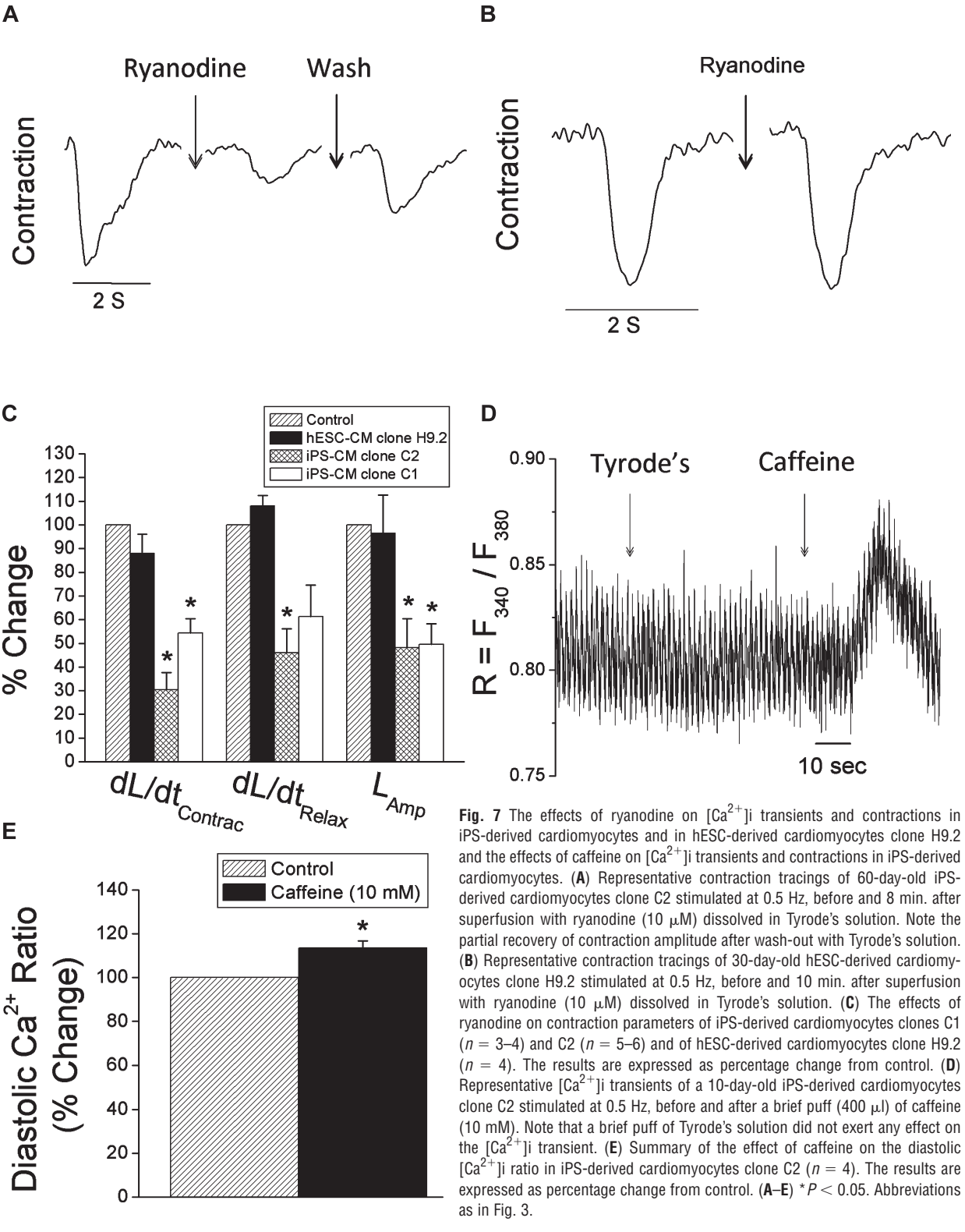

Fig. 7 The effects of ryanodine on $[Ca^{2+}]$i transients and contractions in iPS-derived cardiomyocytes and in hESC-derived cardiomyocytes clone H9.2 and the effects of caffeine on $[Ca^{2+}]$i transients and contractions in iPS-derived cardiomyocytes. (**A**) Representative contraction tracings of 60-day-old iPS-derived cardiomyocytes clone C2 stimulated at 0.5 Hz, before and 8 min. after superfusion with ryanodine (10 μM) dissolved in Tyrode's solution. Note the partial recovery of contraction amplitude after wash-out with Tyrode's solution. (**B**) Representative contraction tracings of 30-day-old hESC-derived cardiomyocytes clone H9.2 stimulated at 0.5 Hz, before and 10 min. after superfusion with ryanodine (10 μM) dissolved in Tyrode's solution. (**C**) The effects of ryanodine on contraction parameters of iPS-derived cardiomyocytes clones C1 (n = 3–4) and C2 (n = 5–6) and of hESC-derived cardiomyocytes clone H9.2 (n = 4). The results are expressed as percentage change from control. (**D**) Representative $[Ca^{2+}]$i transients of a 10-day-old iPS-derived cardiomyocytes clone C2 stimulated at 0.5 Hz, before and after a brief puff (400 μl) of caffeine (10 mM). Note that a brief puff of Tyrode's solution did not exert any effect on the $[Ca^{2+}]$i transient. (**E**) Summary of the effect of caffeine on the diastolic $[Ca^{2+}]$i ratio in iPS-derived cardiomyocytes clone C2 (n = 4). The results are expressed as percentage change from control. (**A**–**E**) $^*P < 0.05$. Abbreviations as in Fig. 3.

© 2011 The Author

Journal of Cellular and Molecular Medicine © 2011 Foundation for Cellular and Molecular Medicine/Blackwell Publishing Ltd

(2) express pluripotent markers as demonstrated by the RT-PCR and immunofluorescence staining (Fig. 1B and C); (3) are capable of differentiating through EB and teratoma formation, while expressing specific markers of the three germ layers (Fig. 1D and E).

The presence of cardiomyocytes within the micro-dissected contracting regions from EBs was established by means of RT-PCR analysis showing that these areas express T-box 5 (Tbx5) and T-box 20 (Tbx20) which are known markers for cardiac mesoderm, as well as the myofilament protein genes cardiac troponin T and α-cardiac actin (Fig. 2A). Further, immunofluorescence analysis of the contracting areas demonstrated that the cells were positive for α-sarcomeric actinin, cardiac troponin I and myosin heavy chain (Fig. 2B). Importantly, in agreement with previous reports on cardiomyocytes derived from mouse and other human iPS clones [11–12, 19], we also found in iPS-CM organized sarcomeric structure.

The basic functional properties of iPS-CM and β-adrenergic responsiveness

As expected, iPS-CM exhibited typical $[Ca^{2+}]_i$ transients and contractions, indicating that the excitation contraction coupling is functional in both clones C1 and C2. Further, the functionality of these cardiomyocytes was further illustrated by the robust extracellular electrograms recorded by means of the MEA data acquisition system. Importantly, analysis of the LAT at each electrode resulted in activation maps with a mean conduction velocity of 10.38 cm/sec. Our ability to successfully record electrograms from confluent networks of iPS-CM and to analyse activation and conduction parameters, will enable us to utilize this unique model for future drug screening. Finally, the resemblance of iPS-CM to hESC-CM [16] is also illustrated by a significant positive inotropic and lusitropic effects of isoproterenol, which were more pronounced in older EBs. The basis for these developmental changes has not been determined in the present study.

Functional properties of iPS-CM

Force–frequency relations

Resembling the behaviour of hESC-CM [15] and contrasted with the adult myocardium (including human heart) [26], iPS-derived cardiomyocytes from both clones display negative FFRs (Fig. 5), which reflect the underlying $[Ca^{2+}]_i$ handling machinery. The final outcome of increased rate of contraction depends on the fine balance between Ca^{2+} influx, SR Ca^{2+} content and release [26, 27]. For either positive or negative FFRs, an increase or decrease in SR Ca^{2+} content and $[Ca^{2+}]_i$ transient amplitude are expected, respectively. Namely, the occurrence of negative or positive FFRs depends on whether the SR releases more Ca^{2+} than it acquires.

Post-rest potentiation in iPS-CM

An important mechanical feature related to a functional SR is PRP. This function is tested by interrupting the regular stimulation with a pause of varying lengths, followed by resumption of the regular stimulation protocol. In principle, due to a larger filling of the SR with Ca^{2+} during the rest, the post-rest contraction is larger than the pre-rest contraction. In essence, while hESC-CM showed no PRP ([15] and present study), iPS-CM exhibited mild potentiation (Fig. 6), albeit with smaller magnitude than in the adult myocardium [15, 28, 29]. Hence, while these findings should be established in iPS from different sources, the preliminary experiments suggest that in the iPS-derived clones investigated in this study, the $[Ca]^{2+}$ handling machinery is probably more mature than that of hESC-CM.

The contribution of SR-Ca^{2+} release to the contraction

Based on the following findings, we concluded that the Ca^{2+}-induced Ca^{2+} release machinery is at least partially functional in iPS-derived cardiomyocytes : (1) These cells exhibit mild PRP; (2) Ryanodine which causes a negative inotropic effect in a variety of cardiac preparations, also decreased contraction amplitude, maximal contraction rate and relaxation rate in both iPS-CM clones investigated (Fig. 7); (3) Caffeine which rapidly increases $[Ca^{2+}]_i$ by opening SR Ca^{2+}-channels, caused a small increase in diastolic $[Ca^{2+}]_i$ in both clones (Fig. 7).

To further test the $[Ca]^{2+}$ handling machinery in iPS-CM, we determined the immunofluorescence expression of ryanodine and calsequestrin (the latter shown to be absent in hESC-CM) [15, 25]. In addition to its Ca^{2+}-binding capacity, calsequestrin is an important luminal regulator of the ryanodine receptor, thus making this molecule a major player in Ca^{2+} homeostasis that extends beyond its ability to modulate intracellular Ca^{2+} [30, 31]. As indicated in Fig. 2B, iPS-CM express both ryanodine and calsequestrin. This is another important support for the presence of adult-like SR function in the iPS clones investigated here. Hence, these findings not only shed light on the excitation contraction coupling machinery of iPS-CM, but also provide an initial indication on the differences between these cells and hESC-CM.

In summary, in the present study we investigated in iPS-CM the basic functional properties related to $[Ca^{2+}]_i$ handling and contraction, as well the contribution of SR Ca^{2+} release to the excitation contraction coupling. Based on the current findings that these cardiomyocytes exhibit at least partial functional SR, we propose that the clones investigated in this study are more mature than the hESC-CM we presently and previously studied. In view of the apparent compatibility of iPS-CM with adult cardiomyocytes, this novel preparation should be further investigated, and considered as an alternative option for cardiac cell therapy.

Acknowledgements

This work was supported by the Ministry of Science and Technology (MOST), Israel Science Foundation (ISF), the Rappaport Family Institute for Research in the Medical Sciences and The Sohnis Family Stem Cells Center, the Russell Berrie Nanotechnology Institute, Technion.

© 2011 The Author
Journal of Cellular and Molecular Medicine © 2011 Foundation for Cellular and Molecular Medicine/Blackwell Publishing Ltd

References

1. **Wong BW, Rahmani M, Rezai N, *et al*.** Progress in heart transplantation. *Cardiovasc Pathol.* 2005; 14: 176–80.
2. **Hunt SA, Haddad F.** The changing face of heart transplantation. *J Am Coll Cardiol.* 2008; 52: 587–98.
3. **Habib M, Caspi O, Gepstein L.** Human embryonic stem cells for cardiomyogenesis. *J Mol Cell Cardiol.* 2008; 45: 462–74.
4. **Segers VF, Lee RT.** Stem-cell therapy for cardiac disease. *Nature.* 2008; 451: 937–42.
5. **Passier R, van Laake LW, Mummery CL.** Stem-cell-based therapy and lessons from the heart. *Nature.* 2008; 453: 322–9.
6. **Dowell JD, Rubart M, Pasumarthi KB, *et al*.** Myocyte and myogenic stem cell transplantation in the heart. *Cardiovasc Res.* 2003; 58: 336–50.
7. **Ménard C, Hagège AA, Agbulut O, *et al*.** Transplantation of cardiac-committed mouse embryonic stem cells to infarcted sheep myocardium: a preclinical study. *Lancet.* 2005; 366: 1005–12.
8. **Laflamme MA, Gold J, Xu C, *et al*.** Formation of human myocardium in the rat heart from human embryonic stem cells. *Am J Pathol.* 2005; 167: 663–71.
9. **Takahashi K, Yamanaka S.** Induction of pluripotent stem cells from mouse embryonic and adult fibroblasts cultures by defined factors. *Cell.* 2006; 126: 663–76.
10. **Takahashi K, Tanabe K, Ohnuki M, *et al*.** Induction of pluripotent stem cells from adult human fibroblasts by defined factors. *Cell.* 2007; 131: 861–72.
11. **Zhang J, Wilson GF, Soerens AG, *et al*.** Functional cardiomyocytes derived from human induced pluripotent stem cells. *Circ Res.* 2009; 104: e30–41.
12. **Tanaka T, Tohyama S, Murata M, *et al*.** *In vitro* pharmacologic testing using human induced pluripotent stem cell-derived cardiomyocytes. *Biochem Biophys Res Commun.* 2009; 385: 497–502.
13. **Xu C, Inokuma MS, Denham J, *et al*.** Feeder-free growth of undifferentiated human embryonic stem cells. *Nat Biotechnol.* 2001; 19: 971–4.
14. **Thomson JA, Itskovitz-Eldor J, Shapiro SS, *et al*.** Embryonic stem cell lines derived from human blastocysts. *Science.* 1998; 282: 1145–7.
15. **Dolnikov K, Shilkrut M, Zeevi-Levin N, *et al*.** Functional properties of human embryonic stem cell-derived cardiomyocytes: intracellular Ca^{2+} handling and the role of sarcoplasmic reticulum in the contraction. *Stem Cells.* 2006; 24: 236–45.
16. **Sedan O, Dolnikov K, Zeevi-Levin N, *et al*.** 1,4,5-Inositol trisphosphate-operated intracellular Ca^{2+} stores and angiotensin-II/endothelin-1 signaling pathway are functional in human embryonic stem cell-derived cardiomyocytes. *Stem Cells.* 2008; 26: 3130–8.
17. **Meiry G, Reisner Y, Feld Y, *et al*.** Evolution of action potential propagation and repolarization in cultured neonatal rat ventricular myocytes. *J Cardiovasc Electrophysiol.* 2001; 12: 1269–77.
18. **Reisner Y, Meiry G, Zeevi-Levin N, *et al*.** Impulse conduction and gap junctional remodelling by endothelin-1 in cultured neonatal rat ventricular myocytes. *J Cell Mol Med.* 2009; 13: 562–73.
19. **Mauritz C, Schwanke K, Reppel M, *et al*.** Generation of functional murine cardiac myocytes from induced pluripotent stem cells. *Circulation.* 2008; 118: 507–17.
20. **Pieske B, Sütterlin M, Schmidt-Schweda S, *et al*.** Diminished post-rest potentiation of contractile force in human dilated cardiomyopathy. Functional evidence for alterations in intracellular Ca2+ handling. *J Clin Invest.* 1996; 98: 764–76.
21. **Bers DM.** Cardiac excitation-contraction coupling. *Nature.* 2002; 415: 198–205.
22. **Poindexter BJ, Smith JR, Buja LM, *et al*.** Calcium signaling mechanisms in dedifferentiated cardiac myocytes: comparison with neonatal and adult cardiomyocytes. *Cell Calcium.* 2001; 30: 373–82.
23. **Liu J, Lieu DK, Siu CW, *et al*.** Facilitated maturation of Ca^{2+} handling properties of human embryonic stem cell-derived cardiomyocytes by calsequestrin expression. *Am J Physiol Cell Physiol.* 2009; 297: C152–9.
24. **Balaguru D, Haddock PS, Puglisi JL, *et al*.** Role of the sarcoplasmic reticulum in contraction and relaxation of immature rabbit ventricular myocytes. *J Mol Cell Cardiol.* 1997; 29: 2747–57.
25. **Liu J, Fu JD, Siu CW, *et al*.** Functional sarcoplasmic reticulum for calcium handling of human embryonic stem cell-derived cardiomyocytes: insights for driven maturation. *Stem Cells.* 2007; 25: 3038–44.
26. **Pieske B, Kretschmann B, Meyer M, *et al*.** Alterations in intracellular calcium handling associated with the inverse force-frequency relation in human dilated cardiomyopathy. *Circulation.* 1995; 92: 1169–78.
27. **Endoh M.** Force-frequency relationship in intact mammalian ventricular myocardium: physiological and pathophysiological relevance. *Eur J Pharmacol.* 2004; 500: 73–86.
28. **Bers DM, Bassani RA, Bassani JW, *et al*.** Paradoxical twitch potentiation after rest in cardiac muscle: increased fractional release of SR calcium. *J Mol Cell Cardiol.* 1993; 25: 1047–57.
29. **Ferraz SA, Bassani JW, Bassani RA**. Rest-dependence of twitch amplitude and sarcoplasmic reticulum calcium content in the developing rat myocardium. *J Mol Cell Cardiol.* 2001; 33: 711–22.
30. **Terentyev D, Viatchenko-Karpinski S, Györke I, *et al*.** Calsequestrin determines the functional size and stability of cardiac intracellular calcium stores: mechanism for hereditary arrhythmia. *Proc Natl Acad Sci USA.* 2003; 100: 11759–64.
31. **Knollmann B.** New roles of calsequestrin and triadin in cardiac muscle. *J Physiol.* 2009; 587: 3081–7.

© 2011 The Author
Journal of Cellular and Molecular Medicine © 2011 Foundation for Cellular and Molecular Medicine/Blackwell Publishing Ltd